Measurement 181 (2021) 109641

Contents lists available at ScienceDirect

Measurement

journal homepage: www.elsevier.com/locate/measurement

Performance of acicular grindable thermocouples for temperature measurements at sliding contacts

Oleksii Nosko [a,*], Wojciech Tarasiuk [a], Yurii Tsybrii [a], Andrey Nosko [b], Adolfo Senatore [c], Veronica D'Urso [c]

[a] Bialystok University of Technology, Faculty of Mechanical Engineering, ul. Wiejska 45C, Bialystok 15351, Poland
[b] Bauman Moscow State Technical University, Department of Lifting and Transport Systems, ul. 2-ya Baumanskaya 5, Moscow 105005, Russia
[c] University of Salerno, Department of Industrial Engineering, via Giovanni Paolo II 132, Fisciano (SA) I84084, Italy

ARTICLE INFO

Keywords:
Grindable thermocouple
Temperature measurement
Contact temperature
Sliding contact

ABSTRACT

The present study investigates the performance of acicular grindable thermocouples based on a constantan wire / steel hollow cylinder construction. The experiments showed that the measuring junction electrical resistance, temperature–voltage characteristic, measuring junction rise time and signal noise standard deviation of the acicular thermocouples are comparable to those of conventional J-type thermocouples with bare wire diameter 0.25–0.5 mm. A pin-on-disc tribometer study of brake friction materials revealed that the acicular thermocouple involved in friction indicates up to 30% higher temperature than the contact temperature rise measured by infrared thermography. Another finding is that the infrared thermography contact temperature can be predicted with significantly higher accuracy by combining the acicular and conventional thermocouple techniques and taking the weighted sum of the respective temperatures.

1. Introduction

Most of the temperature measurements in friction systems use thermoelectric sensors called 'thermocouples' (Komanduri and Hou [1], Davies et al. [2]). A thermocouple in its simplest configuration consists of two dissimilar conductors (electrodes) joined in two junctions. One junction, called 'hot' or 'measuring', is placed inside or on the object under study, while the other junction, called 'cold', is placed in a medium of known temperature. If the temperature of the measuring junction differs from that of the cold junction, the thermocouple generates a thermoelectric voltage. The magnitude of the thermoelectric voltage depends on the materials of the electrodes and the temperatures of the junctions. Temperature–voltage characteristics of the standard electrode couples are accurately tabulated (e.g. Powell et al. [3]).

In order to measure temperature at the sliding surface of a friction component, a thermocouple is installed in the friction component so that its measuring junction is located at a minimum possible distance from the sliding surface. If the friction component is intensively worn out, this distance decreases, and at a certain instance the measuring junction gets involved in friction with the counter component, which will inevitably lead to destruction of the measuring junction or serious deterioration in the thermocouple performance. Thereby, conventional thermocouples cannot provide reliable temperature measurements at sliding surfaces under intensive wear conditions.

The mentioned difficulty can be overcome by applying grindable thermocouples. A single pole grindable thermocouple, most probably introduced first by Peklenik [4], represents a thermocouple in which one insulated electrode is installed in a conductive component with its end exposed to the sliding surface, while the second electrode is the component itself, as shown in Fig. 1a. The measuring junction is formed by plastic deformations of the exposed electrode and adjacent material as the result of their frictional interaction with the counter component. Single pole grindable thermocouples have been used in temperature measurements at grinding contacts, as reported by Nee and Tay [5], Rowe et al. [6], Babic et al. [7], Batako et al. [8], Lefebvre et al. [9,10], Barczak et al. [11].

A double pole grindable thermocouple includes two electrodes in its construction, which makes it applicable to a non-conductive component. The electrodes are installed into the component in parallel at a small distance between each other, as shown in Fig. 1b. Like in a single pole grindable thermocouple, the ends of the electrodes are exposed to the sliding surface and form the measuring junction by undergoing plastic deformations. Thus, the measuring junction is continuously located in

* Corresponding author.
E-mail address: o.nosko@pb.edu.pl (O. Nosko).

https://doi.org/10.1016/j.measurement.2021.109641
Received 12 March 2021; Received in revised form 14 May 2021; Accepted 21 May 2021
Available online 28 May 2021

Nomenclature

Notation

d	diameter of wire electrode of acicular thermocouple, mm
f_c	cutoff frequency of low-pass filter, Hz
f_s	sampling frequency, Hz
t	time variable, s
w	linear wear rate, μm/s
D	outer diameter of hollow cylinder electrode of acicular thermocouple, mm
D_i	inner diameter of hollow cylinder electrode of acicular thermocouple, mm
F	friction force, N
R	electrical resistance of measuring junction, Ω
T	temperature measured by thermocouple, °C
T_e	environment temperature, T_e=20 ± 2 °C
T_w	heated water temperature, T_w=95 ± 5 °C
T_{disc}	disc sample temperature rise measured by infrared thermography, °C
T_{AGT}	contact temperature measured by acicular thermocouple, °C
T_{IR}	contact temperature rise measured by infrared thermography, °C
T_{KT08}	temperature measured by conventional thermocouple KT08, °C
U	thermoelectric voltage of thermocouple, mV
δ	linear wear, μm
σ	standard deviation of thermoelectric voltage U, μV
τ	rise time of measuring junction, ms
AGT41	acicular thermocouple with working part diameter 0.41 mm
AGT46	acicular thermocouple with working part diameter 0.46 mm
JT13	J-type thermocouple with bare wire diameter 0.13 mm
JT25	J-type thermocouple with bare wire diameter 0.25 mm
JT50	J-type thermocouple with bare wire diameter 0.5 mm
KT08	K-type thermocouple with bare wire diameter 0.08 mm

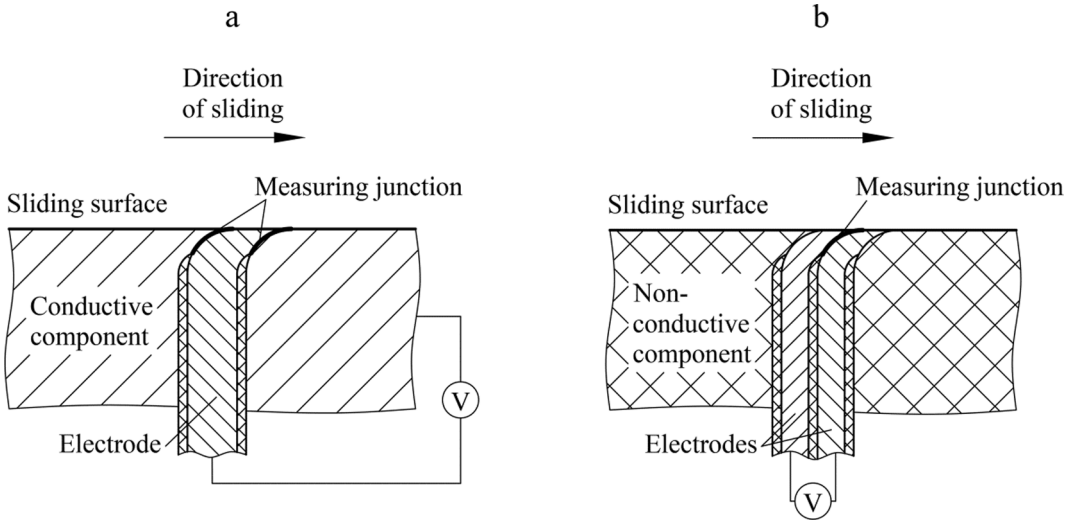

Fig. 1. Grinding thermocouple: (a) single pole construction; (b) double pole construction.

Table 1
Overview of the studies on double pole grindable thermocouples.

Literature source	Materials of electrodes	Geometry of electrodes	Friction component
Braun et al. [12]	Chromel–alumel, chromel–copel	Wires of diameter 0.5 mm	Rubber-based brake lining of train
Guskov [13]	Chromel–copel	Foils of thickness 30 μm	Brake pad of car
Romashko [14]	Chromel–copel	Foils of thickness 20 μm	Brake pad of lift-and-transport machine
Nee and Tay [5]	Chromel–constantan	Foils of thickness ~ 0.2 mm	Steel ground workpiece
Nosko et al. [15]	Chromel–alumel	Foils of thickness 60 μm	Pin sample of brake pad of motor vehicle
	Chromel–copel	Foils of thickness 20 μm	Pin sample of brake pad of lift-and-transport machine

the contact region despite the wear of the friction component.

Double pole grindable thermocouples found their application for measuring temperatures at sliding contacts. Braun et al. [12] investigated grindable thermocouples with electrodes in the form of 0.5 mm diameter wires as applied to train brakes. Guskov [13] measured the surface temperature of a brake pad in contact with a grinding wheel using grindable thermocouples with 30 μm foil electrodes. Romashko [14] made use of grindable thermocouples with 20 μm foil electrodes for the thermal analysis of brakes of lift-and-transport machines. Nosko et al. [15] performed a pin-on-disc study of grindable thermocouples with 60 μm and 20 μm foil electrodes as applied to brake materials of motor vehicles. Table 1 overviews the relevant studies and thermocouple characteristics.

Analysis of the literature sources above shows that the shapes of grindable thermocouple electrodes are limited mainly to foils and rectangular cross-section rods. Installation of an ensemble of two such electrodes requires the following steps: cutting out of a piece of material from the friction component; splitting of the piece in two parts; milling of a groove in one of the parts; placement of the working part of the grindable thermocouple into the groove; assembling of the two parts

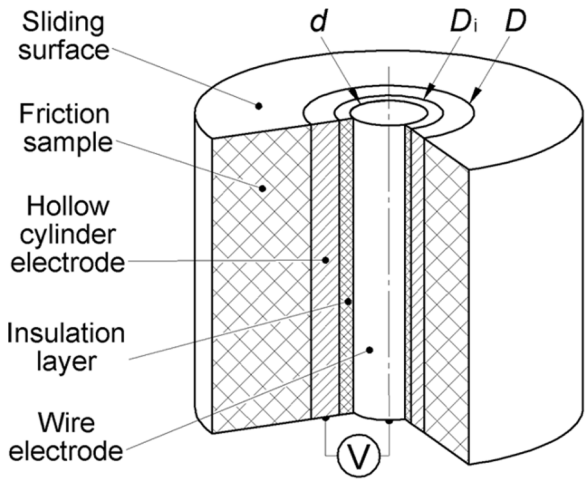

Fig. 2. Schematic of the working part of acicular thermocouple.

Table 2
Geometric parameters of the electrodes.

Acicular thermocouple	D, mm	D_i, mm	d, mm
AGT41	0.41	0.21	0.08
AGT46	0.46	0.26	0.13

Table 3
Elemental compositions of the steel and constantan electrodes, wt%.

Electrode	C	O	P	Cr	Mn	Fe	Ni	Cu
Steel (hollow cylinder)	2.8	4	0.8	17.7	1.6	65	8.1	
Constantan (wire)	7.9	0.7			1.1		39.8	50.5

back to a single piece; placement of the piece in its initial place in the friction component. Thereby, the foil construction of grindable thermocouples is not feasible in terms of installation. A solution that could potentially eliminate the mentioned disadvantage is the application of acicular grindable thermocouples based on a wire-in-hollow-cylinder construction. Similar thermocouples, though possessing unaltered measuring junctions, are employed in aerodynamic and hydrodynamic measurements (Mohammed et al. [16], Irimpan et al. [17], Agarwal et al. [18], Li et al. [19], Manjhi and Kumar [20,21]). With this in mind, the purpose of the present study was to experimentally investigate the performance characteristics of acicular thermocouples as applied to brake friction materials and compare the acicular thermocouple measurements to those performed by conventional thermocouples and infrared thermography.

2. Construction and installation of acicular thermocouples

The working (wearable) part of an acicular thermocouple comprises a hollow cylinder electrode and a wire electrode with an insulation layer, as illustrated in Fig. 2. The hollow cylinder electrode is characterised by its outer diameter D and inner diameter D_i. The wire electrode has diameter d. The present study focusses on the investigation of two types of acicular thermocouples code-named AGT41 and AGT46. The parameters of their electrodes are presented in Table 2.

The working part of the acicular thermocouple was assembled in the following manner. The wire electrode covered by an insulation layer was carefully inserted into the hollow cylinder electrode of length 10 mm. The outer diameter of the insulation layer was slightly smaller than D_i, providing the radial gap between the hollow cylinder electrode and insulation layer below 20 μm. The measuring junction end of the working part was ground. The wire electrode coming out from the

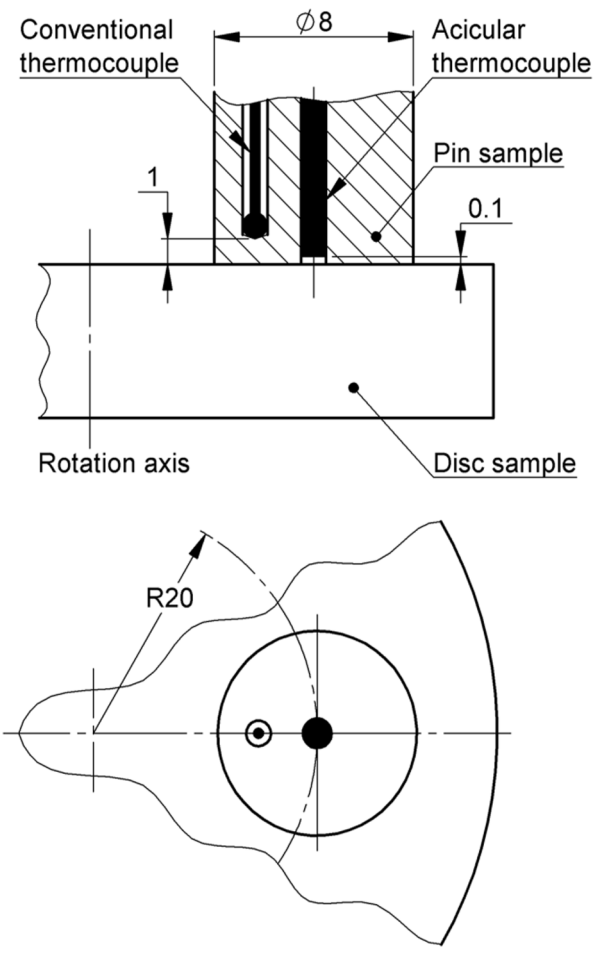

Fig. 3. Initial locations of the acicular and conventional thermocouples in the pin sample.

reverse end of the working part was glued to the hollow cylinder electrode.

The hollow cylinder electrode was made of steel, while the wire electrode was made of constantan. The material of the insulation layer was perfluoroalkoxy. The elemental compositions of the electrodes obtained by energy-dispersive X-ray spectroscopy are presented in Table 3.

The installation of the acicular thermocouple into a friction sample included drilling of a hole in the friction sample perpendicular to the sliding surface, insertion of the working part of the acicular thermocouple into the hole so that its measuring junction end was exposed to the sliding surface, fixation of the working part by gluing its reverse end to the friction sample. It is apparent that the mentioned installation procedure is substantially simpler compared to that described in Section 1 for a foil-construction grindable thermocouple.

3. Pin-on-disc research methodology

The tests were performed on a T11 pin-on-disc tribometer. The pin sample had diameter 8 mm and height 8 mm. An acicular thermocouple with a premade measuring junction was installed into the pin sample along its axis, as shown in Fig. 3. There was an initial gap of about 0.1 mm between the working part of the acicular thermocouple and the sliding surface. Moreover, a conventional K-type thermocouple with bare wire diameter 0.08 mm, code-named KT08, was installed into a 0.6 mm diameter blind hole in the pin sample. The initial distance between the measuring junction of KT08 and the sliding surface was 1 mm. The temperature signals from the acicular thermocouple and KT08, denoted by respective T_{AGT} and T_{KT08}, were sampled at frequency $f_s = 1$ Hz and

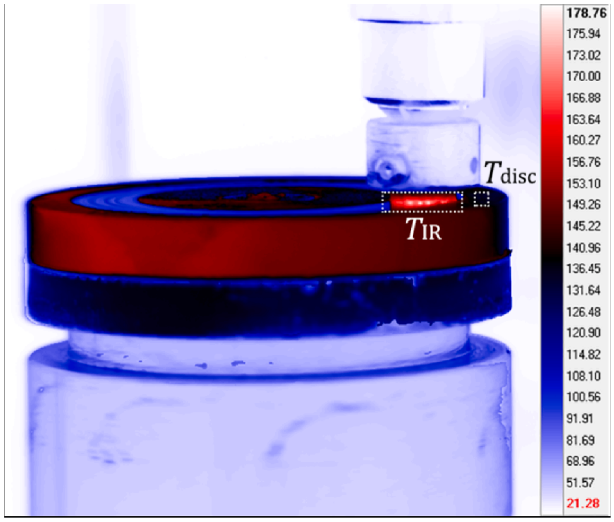

Fig. 4. Thermal image obtained by infrared thermography (AGT41, 1 MPa × 2 m/s).

low-pass filtered with cutoff frequency $f_c = 1.5$ Hz by a Graphtech GL7000/GL7-HSV data logger.

The pin sample was pressed against a disc sample by a dead weight. The disc sample had diameter 60 mm and thickness 6.5 mm. The average friction radius, i.e. the distance between the axes of the pin and disc samples, was 20 mm. The friction force F was measured by an HBM S2 force transducer with resolution 0.01 N. The linear wear δ of the pin and disc samples was measured by an HBM WI inductive displacement transducer with resolution 0.1 μm.

Pin samples were milled out from the friction pads of a car brake using a 6040T4D numerically controlled milling machine. The material of the friction pads belonged to the class of low-metallic materials. Disc samples were manufactured from 42CrMo4 tribological steel of hardness HV190. The friction surfaces of the disc samples were ground to have Ra1.6.

The tests were done under four stationary friction regimes, namely 0.5 MPa × 1 m/s, 0.5 MPa × 2 m/s, 1 MPa × 1 m/s, 1 MPa × 2 m/s. The nominal contact pressure in MPa is equal to the ratio of the axial force on the pin sample to the nominal contact area. The sliding velocity in m/s corresponds to the average friction radius.

The temperatures of the pin and disc samples were also measured by a Cedip Titanium 560 M infrared thermographic camera with detector spectral range 3.6–5.1 μm, thermal sensitivity 20 mK and resolution 640 × 512 pixels. The disc sample was sprayed with carbon black paint with emissivity 0.96. The thermographic camera was focussed on the visible part of the pin sample, as illustrated in Fig. 4. A thermal image was taken every 30 min during the test. The spatial resolution of the thermal image was 0.12 mm. Analysis of the thermal image allowed to determine maximum temperature rise T_{IR} in the region of visible contact and the temperature rise T_{disc} of the disc sample in the vicinity of the contact region. Note that the thermographic camera underestimates the temperature of the wear track on the disc sample due to a lower emissivity of the steel surface compared to that of the carbon black paint.

4. Results and discussion

4.1. Measuring junction electrical resistance

When an acicular thermocouple is involved in friction with a counter component, its working part is continuously deformed and worn out by roughness asperities of the counter component. Fig. 5 shows the typical images of the measuring junction end of the working part before a pin-on-disc test (a) and the worn measuring junction end after the test (b). It is easily seen that after the test there are friction tracks passing through the central region of the measuring junction end. These friction tracks connect the electrodes of the acicular thermocouple forming its measuring junction.

The shape and size of the measuring junction have a decisive influence on the grindable thermocouple performance. The electrical resistance R of the measuring junction allows estimating its overall volume (Lefebvre et al. [9]). In general, a smaller value of R corresponds to a larger measuring junction, slower thermocouple response and more stable signal. The values of R of the worn acicular thermocouples AGT41 and AGT46 were systematically investigated. The measurements were performed by a digital multimeter with resolution 0.01 Ω at environment temperature $T_e = 20 \pm 2$ °C. In each measurement, the test leads of the multimeter were connected to the hollow cylinder electrode and the wire electrode coming out from the reverse end of the working part of the acicular thermocouple. For the sake of comparisons, the measurements of R were also done for new conventional J-type thermocouples with respective bare wire diameters 0.13, 0.25, 0.5 mm and measuring junction diameters 0.19, 0.29, 0.66 mm, code-named JT13, JT25, JT50.

Fig. 6 illustrates the measurement results for all thermocouple types. The bars indicate the mean values of R, while the line segments indicate the standard deviation ranges of R. It is seen that the arrangement of the conventional thermocouples in ascending order of R, namely JT50 → JT25 → JT13, corresponds to decreasing in the size of the measurement junction. In terms of R, AGT46 with $R \approx 14$ Ω is between JT50 and JT25, while AGT41 with $R \approx 32$ Ω is between JT25 and JT13. It is also seen that the dispersions of R of the conventional thermocouples associated with

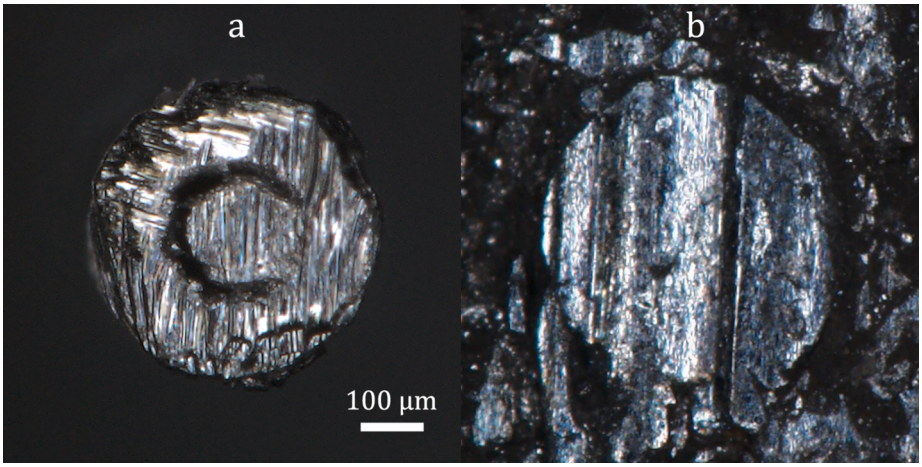

Fig. 5. Measuring junction end of AGT46 before (a) and after (b) a pin-on-disc test.

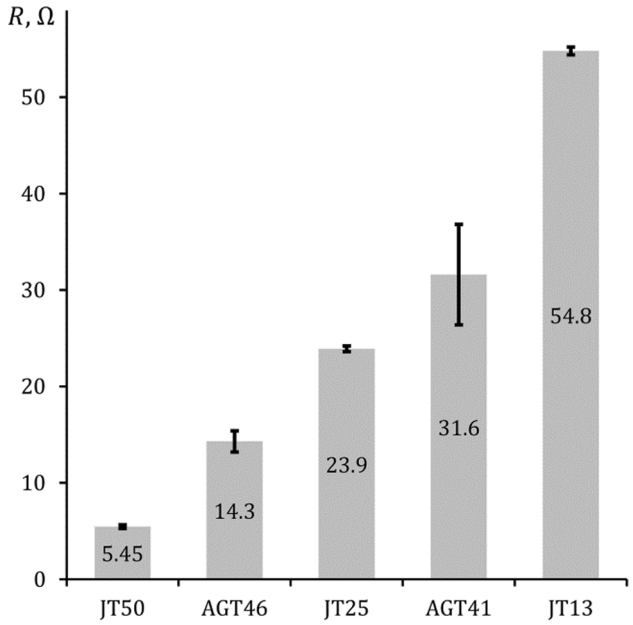

Fig. 6. Mean value and standard deviation range of the electrical resistance R.

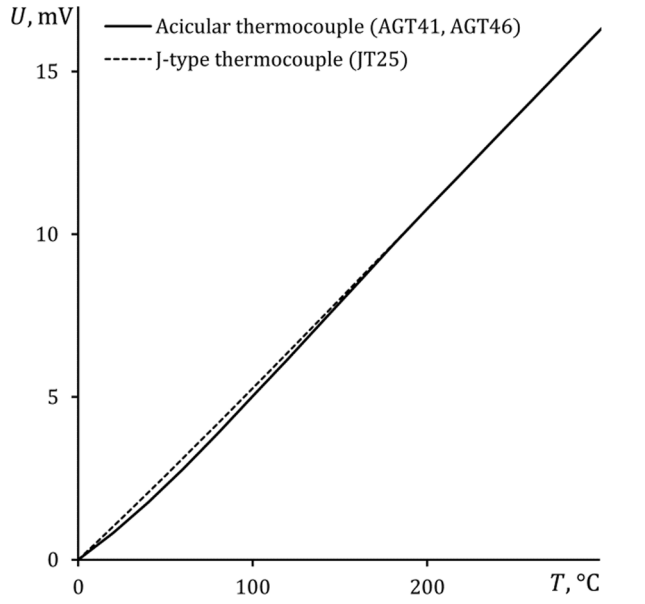

Fig. 8. Relationship between the measured temperature T and thermoelectric voltage U.

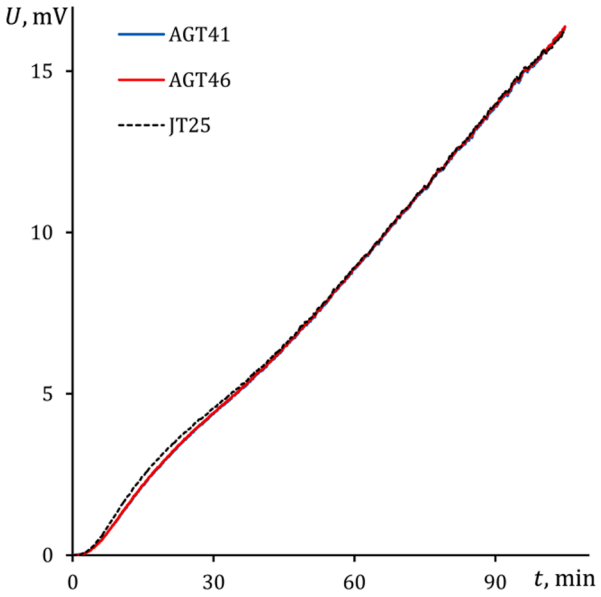

Fig. 7. Thermoelectric voltage U generated by AGT41, AGT46 and JT25.

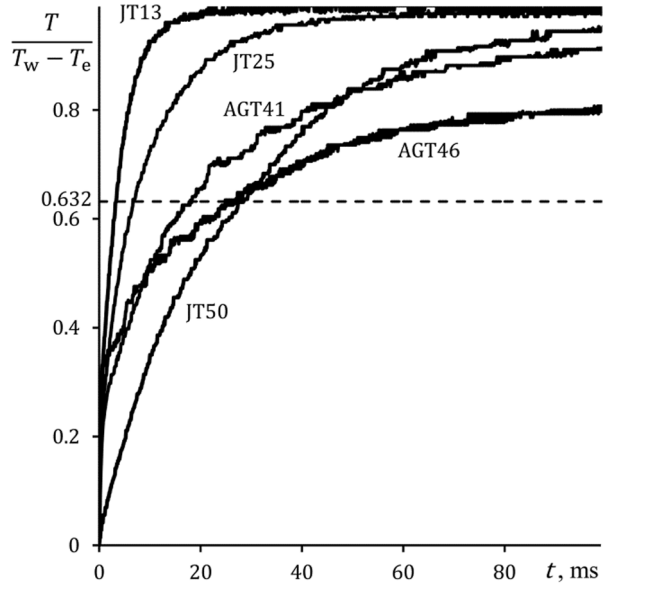

Fig. 9. Response of the measured temperature T to the step-wise change $(T_w - T_e)$.

the measurement repetitions are small. By contrast, AGT41 and AGT46 have significantly larger dispersions of R, which can be explained by variations in the shape and size of the measuring junction due to differing regimes of the pin-on-disc tests and random mechanical processes at the sliding contact.

4.2. Temperature–voltage characteristic

Application of a thermocouple requires the knowledge of its temperature–voltage characteristic, i.e. the relationship between the measured temperature T and thermoelectric voltage U. The temperature–voltage characteristics of the acicular thermocouples were investigated using a Maytec electric furnace controlled by a Zwick/Roell unit. The measuring junctions of the worn acicular thermocouples AGT41 and AGT46 and a well-calibrated conventional thermocouple JT25 were placed inside the furnace. Temperature in the furnace increased from T_e to 320 °C with rate 3 °C/min. The signals from the thermocouples were recorded by the data logger. The described procedure was conducted 3 times for each set of thermocouples.

Fig. 7 shows the typical increase in the thermocouple signals. According to the presented results, AGT41 and AGT46 generate almost identical thermoelectric voltages. The difference between them is hardly distinguishable. The temperature–voltage characteristic of AGT41 and AGT46 was determined based on the known characteristic of JT25 which is in very close agreement with the thermocouple reference tables by Powell et al. [3]. Fig. 8 shows that the obtained temperature–voltage characteristic of the acicular thermocouple deviates from that of the J-type thermocouple on the interval of 0 to about 150 °C, while they practically coincide on the interval of 150 to 300 °C. The mentioned deviation is most probably related to the fact that the steel electrode of the acicular thermocouple contains non-iron content, mainly Cr and Ni

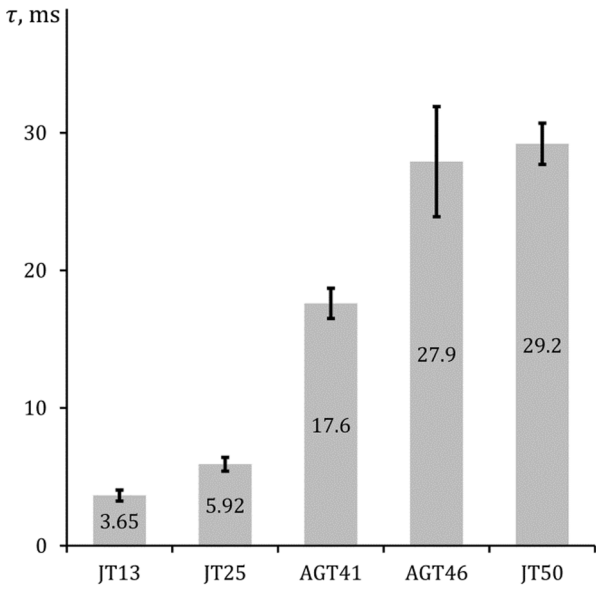

Fig. 10. Mean value and standard deviation range of the measuring junction rise time τ.

(see Table 3).

4.3. Measuring junction rise time

In the present study, the measuring junction of a thermocouple is characterised by the rise time τ indicating how fast it responds to a step-wise change in the ambient temperature and reaches the level of 63.2% of its stationary value. The value of τ was estimated by rapid immersion of the measuring junction in water at temperature $T_w = 95 \pm 5$ °C. The measured temperature T increased thereby from zero to the relative water temperature $(T_w - T_e)$. The temperature signal was sampled by the data logger at frequency$f_s = 10$ kHz.

Fig. 9 illustrates the typical temperature responses of the worn acicular thermocouples AGT41 and AGT46 and conventional thermocouples JT13, JT25 and JT50. In the case of JT13, JT25 or JT50, T increases almost in an exponential manner. On the other hand, T of either of AGT41 and AGT46 undergoes a sudden rise and then increases with a significantly lower rate lagging behind JT13, JT25 and eventually JT50. The mentioned difference in the thermal behaviour can be explained by that the measuring junction of the conventional thermocouple has spherical shape and, therefore, behaves due to a point heat capacitance model. The working part of the acicular thermocouple represents an elongated cylinder with a measuring junction at its end. Accordingly, the initial sudden rise of T is most probably attributed to the direct contact of the measuring junction with water, while the subsequent behaviour of T is governed by heat conduction in the working part.

The procedure described above was conducted 10 times for each thermocouple. The relevant statistical data are shown in Fig. 10. According to these data, $\tau \approx 18$ ms of AGT41 is shorter than $\tau \approx 28$ ms of AGT46, which is due to the smaller size of AGT41 (see Table 2). As compared to the conventional thermocouples, AGT41 and AGT46 respond significantly slower than JT13 and JT25.

4.4. Thermocouple signal noise

The signal of a thermocouple is strongly affected by imperfections of its measuring junction, measurement system parameters and environmental electromagnetic fields (Batako et al. [8]). One of the efficient tools to eliminate the undesired component (noise) of the signal is low-pass filtering. With this in mind, the influence of the cutoff frequency f_c of the data logger low-pass filter was investigated. The thermoelectric voltage U of the studied thermocouple was sampled for the interval of 100 s at frequency $f_s = 10$ Hz. Based on the measurement data, U was characterised by its standard deviation σ. The measurement conditions were the same for all studied thermocouples including the input channel of the data logger, settings of the data logger, relative position of the electrical devices and wires, environment temperature.

Fig. 11 shows the values of σ obtained for the worn acicular thermocouples AGT41 and AGT46 and conventional thermocouples JT13, JT25, JT50 at different values of f_c. It is seen that at f_c equal to 1.5, 5, 50, 500 or 5 k Hz, σ is below 10 μV and exhibits no particular trends related to the thermocouple type or change in f_c. As f_c is switched from 5 kHz to 50 kHz or from 50 kHz to 'no filter' mode, σ becomes larger. For $f_c = 50$ kHz and 'no filter' mode, all thermocouples have close values of σ, except for JT13 which has about twice as larger σ. The obtained results suggest that JT13 generates a more unstable signal, which correlates with its larger value of R (see Fig. 6). Similar results were also confirmed for $f_s = 1$ Hz and $f_s = 100$ Hz. Thereby, AGT41 and AGT46 are comparable to JT25 and JT50 in terms of σ.

4.5. Acicular thermocouple accuracy

Fig. 12 presents the typical results obtained from a single pin-on-disc test. The left plot shows the friction force F and linear wear δ, while the right one shows the temperatures T_{AGT}, T_{KT08}, T_{IR} and T_{disc}. On the interval from zero to about 60 min, one can clearly see the running-in processes associated with contact area growth, temperature increase, formation of the stationary roughness and other factors. Further, on the

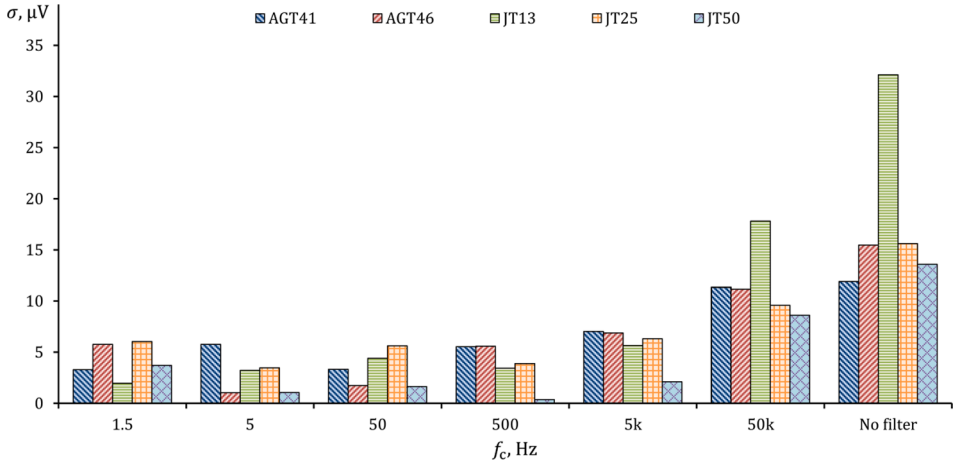

Fig. 11. Standard deviation σ of the thermoelectric voltage U vs low-pass filter cutoff frequency f_c.

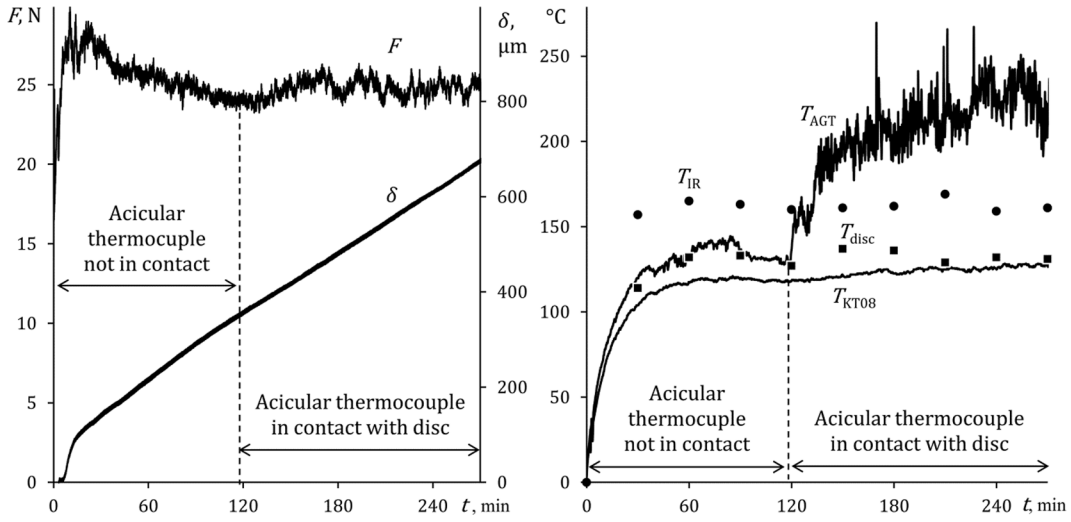

Fig. 12. Typical test results (AGT41, 1 MPa × 2 m/s).

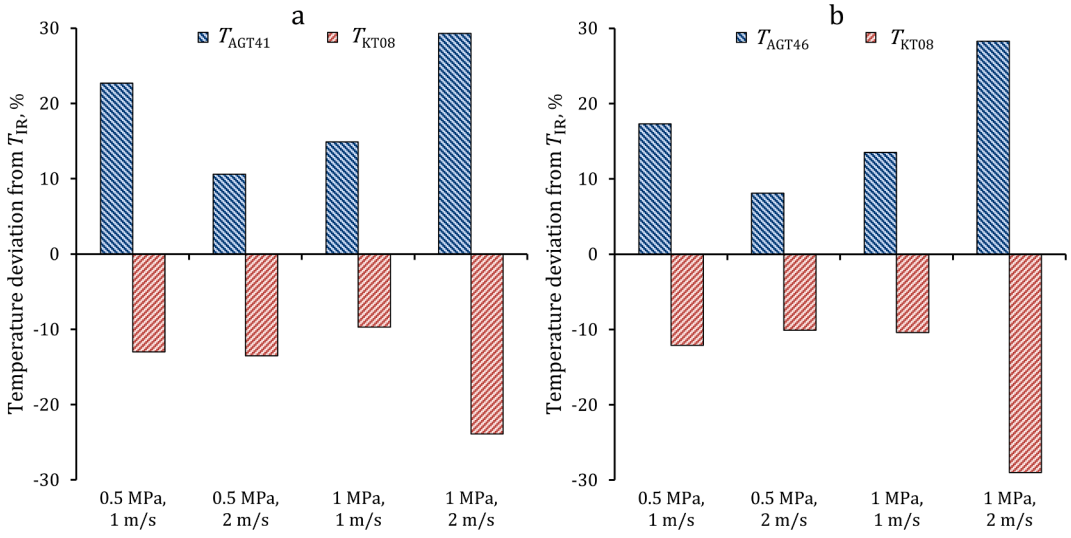

Fig. 13. Deviations of the temperatures T_{AGT} and T_{KT08} from T_{IR}: (a) AGT41; (b) AGT46.

interval from 60 min to 120 min, the pin sample is steadily worn out, resulting in a decrease in the gap between the working part of the acicular thermocouple and the sliding surface. At the time instance of about 120 min, the working part gets involved in friction with the disc sample. Starting from that instance, the temperature T_{AGT} measured by the acicular thermocouple behaves in a qualitatively different manner.

The experimental data obtained under the four friction regimes suggest that the acicular thermocouple uninvolved in friction (see the interval 30–120 min in Fig. 12) indicates the temperature T_{AGT} which practically coincides with the disc sample temperature T_{disc}. On this interval, the temperature T_{KT08} measured by the conventional thermocouple KT08 is lower than T_{AGT}, whereas the temperature rise T_{IR} measured by the thermographic camera is noticeably higher. After the acicular thermocouple got involved in friction, T_{AGT} exceeds T_{IR}, which is caused by excessive generation of friction heat in the contact region between the working part of the acicular thermocouple and the disc sample (Nosko et al. [15]). The measuring junction of the acicular thermocouple being directly involved in the frictional interaction undergoes multiple deformations, resulting in the oscillatory component of T_{AGT} (Lefebvre et al. [10]). It is notable that the frequency spectrum analysis revealed no correlations between the readings of T_{AGT} and the friction force F. The temperatures T_{IR}, T_{disc} and T_{KT08} exhibit a relatively stable behaviour, although the latter one has an increasing trend due to the wear of the pin sample.

The accuracy of the thermocouple measurements was evaluated with respect to T_{IR}. Fig. 13 shows the percent deviations of the temperatures T_{AGT} and T_{KT08} from T_{IR}. The deviation of T_{AGT} was determined by averaging T_{AGT} and T_{IR} over the last 60 min of the test when the working part of the acicular thermocouple is completely involved in friction. The deviation of T_{KT08} was determined by averaging T_{KT08} and T_{IR} over the 60 min interval corresponding to about 0.5 mm distance between the measuring junction of KT08 and the sliding surface. This interval was identified from the time dependency of the linear wear δ (see Fig. 12). It is apparent that T_{IR} is systematically overestimated by T_{AGT} and underestimated by T_{KT08}. Note that the relationship between T_{AGT} and the friction regime is similar for AGT41 (Fig. 13a) and AGT46 (Fig. 13b). The maximum deviation of T_{AGT} that makes up about 30% corresponds to the most intensive friction regime of 1 MPa × 2 m/s, while its minimum deviation of about 10% corresponds to the friction regime 0.5 MPa × 2 m/s of average intensity in terms of friction power.

It is interesting to analyse how accurately one can predict T_{IR} by taking the weighted sum of T_{AGT} and T_{KT08}. The weight coefficients are chosen so as to minimise the absolute deviation of the weighted sum from T_{IR} for all friction regimes. Fig. 14 presents the percent deviations

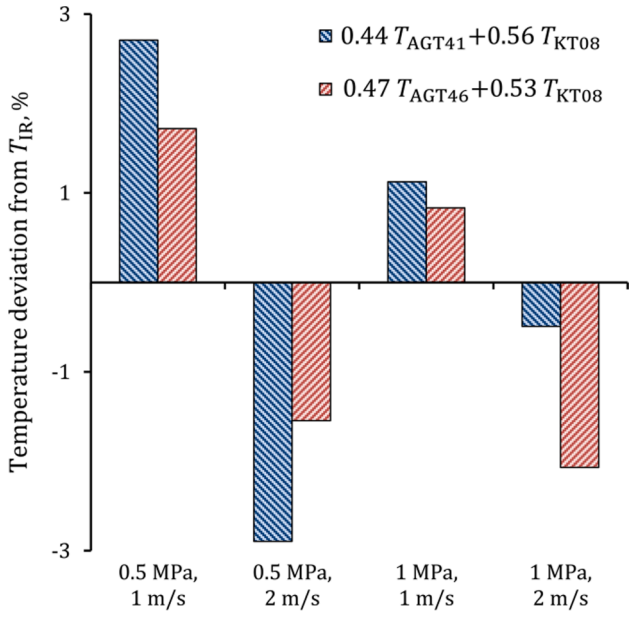

Fig. 14. Deviation of the optimum normalised weighted sum of T_{AGT} and T_{KT08} from T_{IR}.

of the optimum normalised weighted sum for each type of acicular thermocouple found based on the data of Fig. 13. In the case of AGT41, the optimum normalised weighted sum of $0.44T_{AGT}+0.56T_{KT08}$ provides absolute deviations below 2.9%. As for AGT46, the optimum normalised weighted sum is $0.47T_{AGT}+0.53T_{KT08}$ at which the absolute deviations are below 2.1%. Thereby, the combination of the acicular and conventional thermocouple techniques allows to significantly increase the prediction accuracy of T_{IR}.

4.6. Acicular thermocouple transparency

The transparency of the acicular thermocouple, i.e. its ability not to alter the processes occurring in the contact region, was characterised in terms of changes in the friction force F and wear rate w. Fig. 15 presents the relevant data. Fig. 15a shows the percent change in F after the acicular thermocouple got involved in friction. The calculation was based on the average values of F over 60 min just before the thermocouple involvement in friction and over the last 60 min of the test. It is seen that the change in F is between −3.9% and 1.5% for both thermocouple types and all friction regimes. Such a small change is comparable to random variations due to inhomogeneity of the material of the pin sample and other factors. Consequently, the frictional interaction of the acicular thermocouple and disc sample has a negligibly small influence on the average level of the friction force F.

The wear rate w was determined as the slope of the time dependency of the linear wear δ. As in the case of friction force, the change in w was calculated based on its averaging over 60 min just before the thermocouple involvement in friction and over the last 60 min of the test. Fig. 15b presents the percent change in w for all friction regimes. There is a significant decrease in w varying between 8% and 18%. This decrease is most probably caused by that the steel hollow cylinder electrode has a higher wear resistance compared to the pin sample material. It is also seen that the largest decrease in w for both thermocouple types takes place at the sliding velocity of 2 m/s. Thereby, the factor of sliding velocity has likely a stronger influence on the change in w than that of contact pressure.

The transparency analysis was finalised by investigating the worn surface of the disc sample. Fig. 16 shows a profile of the worn surface measured in the radial direction by an Olympus Lext OLS4000 Industrial Laser Confocal Microscope. The presented worn surface corresponds to the most intensive friction regime of 1 MPa × 2 m/s. It is shown that the profile of the wear track opposite the pin sample has a noticeably smaller roughness with respect to the initial one. There are several furrows of depth 2–3 μm that are most probably related to non-uniform distribution of metallic content in the pin sample. As regards the impact of the acicular thermocouple, no excessive or abnormal wear at the radius of its location is seen.

5. Conclusions

A comprehensive study of the acicular grindable thermocouples based on a wire-in-hollow-cylinder construction was performed. Two types of steel–constantan acicular thermocouples with working part diameters 0.41 mm and 0.46 mm were developed. The measuring junction characteristics were investigated and compared to those of conventional J-type thermocouples. The accuracy and transparency of the acicular thermocouples were investigated as applied to brake friction materials using a pin-on-disc tribometer. The acicular thermocouple measurements were compared to those done by infrared thermography. The main findings of the study are summarised as follows:

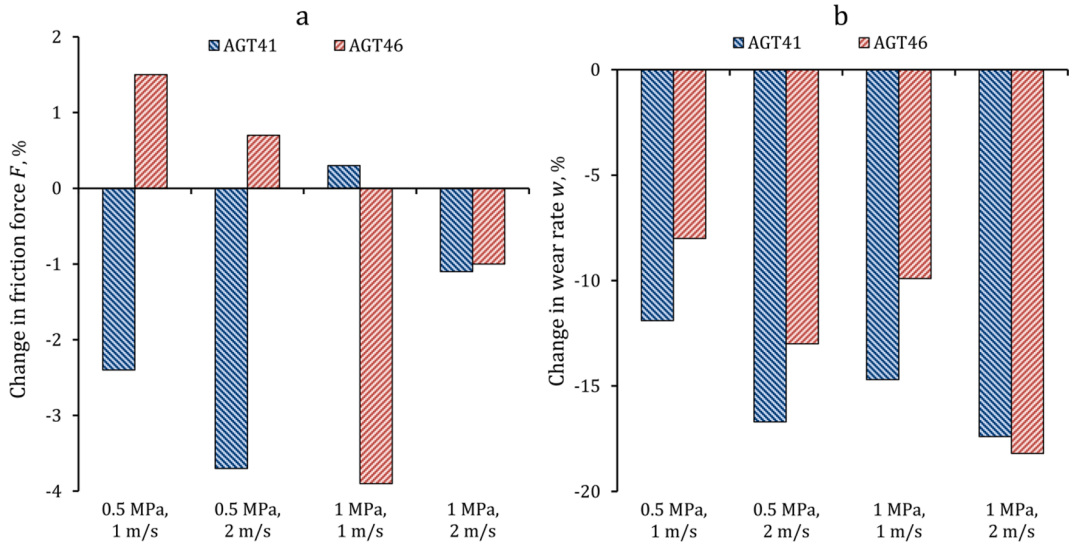

Fig. 15. Influence of the acicular thermocouple on the friction force F (a) and wear rate w (b).

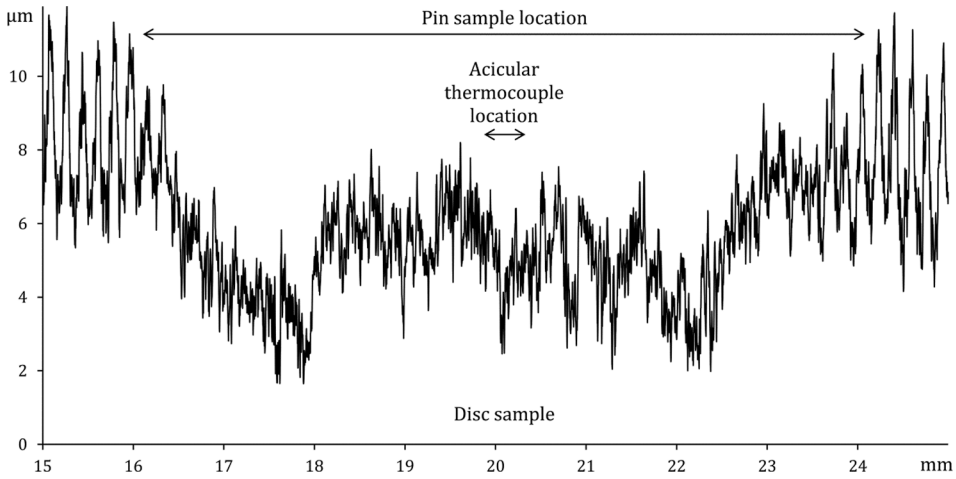

Fig. 16. Radial profile of the worn surface of the disc sample (AGT46, 1 MPa × 2 m/s).

1. Compared to other types of grindable thermocouples, the acicular thermocouple is feasible in installation due to its cylinder-shaped working part.
2. The measuring junction electrical resistance, temperature–voltage characteristic, measuring junction rise time and signal noise standard deviation of the developed acicular thermocouples are generally comparable to those of conventional J-type thermocouples with bare wire diameter 0.25–0.5 mm.
3. The acicular thermocouple involved in friction indicates up to 30% higher temperature than the contact temperature rise measured by infrared thermography.
4. The infrared thermography contact temperature can be predicted with significantly higher accuracy by combining the acicular and conventional thermocouple techniques and taking the weighted sum of the respective temperatures.
5. The acicular thermocouples are transparent in terms of friction force.

CRediT authorship contribution statement

Oleksii Nosko: Funding acquisition, Supervision, Conceptualization, Writing - original draft. **Wojciech Tarasiuk:** Methodology, Visualization, Software. **Yurii Tsybrii:** Investigation, Validation, Writing - review & editing. **Andrey Nosko:** Supervision, Writing - review & editing. **Adolfo Senatore:** Resources, Writing - review & editing. **Veronica D'Urso:** Resources, Writing - review & editing.

Declaration of Competing Interest

The authors declare that there is no conflict of interest.

Acknowledgements

The present work was supported by the National Science Centre, Poland [grant number 2017/26/D/ST8/00142]. The authors wish to thank Dr Magdalena Łępicka, Dr Karol Golak, Dr Adam Adamowicz and Mr Wojciech Grodzki at Bialystok University of Technology for their assistance in conducting experiments.

References

[1] R. Komanduri, Z.B. Hou, A review of the experimental techniques for the measurement of heat and temperatures generated in some manufacturing processes and tribology, Tribol. Int. 34 (10) (2001) 653–682.
[2] M.A. Davies, T. Ueda, R. M'Saoubi, B. Mullany, A.L. Cooke, On the measurement of temperature in material removal processes, Annals of the CIRP 56 (2) (2007) 581–604.
[3] R.L. Powell, W.J. Hall, C.H. Hyink, L.L. Sparks, G.W. Burns, M.G. Scroger, H.H. Plumb, Thermocouple reference tables based on the IPTS-68, National Bureau of Standards Monograph 125, 1974.
[4] J. Peklenik, Ermittlung von geometrischen und physikalischen Kenngrössen für die Grundlagenforschung des Schleifens [dissertation], TH Aachen, 1957, Aachen. (in German).
[5] A.Y.C. Nee, A.O. Tay, On the measurement of surface grinding temperature, Int. J. Mach. Tool Des. Res. 21 (3-4) (1981) 279–291.
[6] W.B. Rowe, S.C.E. Black, B. Mills, H.S. Qi, M.N. Morgan, Experimental investigation of heat transfer in grinding, CIRP Ann. 44 (1) (1995) 329–332.
[7] D. Babic, D.B. Murray, A.A. Torrance, Mist jet cooling of grinding processes, Int. J. Mach. Tools Manuf 45 (10) (2005) 1171–1177.
[8] A.D. Batako, W.B. Rowe, M.N. Morgan, Temperature measurement in high efficiency deep grinding, Int. J. Mach. Tools Manuf 45 (11) (2005) 1231–1245.
[9] A. Lefebvre, P. Vieville, P. Lipinski, C. Lescalier, Numerical analysis of grinding temperature measurement by the foil/workpiece thermocouple method, Int. J. Mach. Tools Manuf 46 (14) (2006) 1716–1726.
[10] A. Lefebvre, F. Lanzetta, P. Lipinski, A.A. Torrance, Measurement of grinding temperatures using a foil/workpiece thermocouple, Int. J. Mach. Tools Manuf 58 (2012) 1–10.
[11] L.M. Barczak, A.D.L. Batako, M.N. Morgan, A study of plane surface grinding under minimum quantity lubrication (MQL) conditions, Int. J. Mach. Tools Manuf 50 (11) (2010) 977–985.
[12] E.D. Braun, P.P. Gushin, V.F. Titarenko, B.A. Shyryaev, Selection of temperature sensor constructions for testing friction brakes, Vestnik VNIIZhT (6) (1972) 60–62 (in Russian).
[13] V.I. Guskov, A new method of temperature measurement in the grinding zone, Russian Eng. J. 6 (1974) 74–75 (in Russian).
[14] A.M. Romashko, Study of heating of lift-and-transport machines disk brakes [dissertation], Bauman Moscow Higher Technical School, 1979, Moscow (in Russian).
[15] O. Nosko, T. Nagamine, A.L. Nosko, A.M. Romashko, H. Mori, Y. Sato, Measurement of temperature at sliding polymer surface by grindable thermocouples, Tribol. Int. 88 (2015) 100–106.
[16] H. Mohammed, H. Salleh, M.Z. Yusoff, Design and fabrication of coaxial surface junction thermocouples for transient heat transfer measurements, Int. Commun. Heat Mass Transfer 35 (7) (2008) 853–859.
[17] K.J. Irimpan, N. Mannil, H. Arya, V. Menezes, Performance evaluation of coaxial thermocouple against platinum thin film gauge for heat flux measurement in shock tunnel, Measurement 61 (2015) 291–298.
[18] S. Agarwal, N. Sahoo, R.K. Singh, Experimental techniques for thermal product determination of coaxial surface junction thermocouples during short duration transient measurements, Int. J. Heat Mass Transf. 103 (2016) 327–335.
[19] J. Li, H. Chen, S. Zhang, X. Zhang, H. Yu, On the response of coaxial surface thermocouples for transient aerodynamic heating measurements, Exp. Therm Fluid Sci. 86 (2017) 141–148.
[20] S.K. Manjhi, R. Kumar, Transient surface heat flux measurement for short duration using K-type, E-type and J-type of coaxial thermocouples for internal combustion engine, Measurement 136 (2019) 256–268.
[21] S.K. Manjhi, R. Kumar, Performance analysis of coaxial thermocouples for heat flux measurement of an aerodynamic model on shock tube facility, Measurement 166 (2020), 108221.